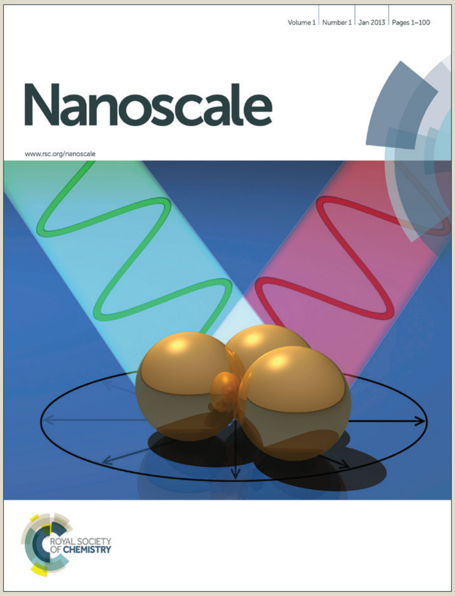
Volume 1 | Number 1 | Jan 2013 | Pages 1–100
Nanoscale
www.rsc.org/nanoscale
ROYAL SOCIETY OF CHEMISTRY

Nanoscale RSCPublishing

COMMUNICATION

Cite this: DOI: 10.1039/x0xx00000x

Received 00th February 2015,
Accepted 00th February 2015

DOI: 10.1039/x0xx00000x

www.rsc.org/nanoscale

Enable Low-Amount YAG:Ce^{3+} to Convert into White Light with Plasmonic Au Nanoparticles

Talib Hussain,[abe] Liubiao Zhong,[b] Mohammad Danesh,[c] Huiqi Ye,[a] Ziqiang Liang,[b] Dong Xiao,[a] Cheng-Wei Qiu,[c] Chaogang Lou,[d] Lifeng Chi,*[b] and Lin Jiang*[b]

Abstract. We report a new strategy to attach Au nanoparticles onto YAG:Ce^{3+} phosphor directly by the chemical preparation method, which yields efficient and quality conversion of blue light to yellow in the presence of low amount of phosphor. PL intensity and quantum yield of YAG:Ce^{3+} phosphor are significantly enhanced after Au nanoparticle modification which can be attributed to strongly enhanced local surface electromagnetic field of Au nanoparticles on phosphor particle surface. The CIE color coordinates move from blue light (0.23, 0.23) to white light region (0.30, 0.33) with CCT value of 6601 K and good white light CRI value of 78, which indicates Au nanoparticles greatly improve the conversion efficiency of low-amount YAG:Ce^{3+} in WLEDs.

The rare-earth doped phosphor crystal YAG (yttrium aluminium garnet) is being widely investigated in the field of solid-state lighting, laser, scintillators and refractive coating, owing to its attractive optical property, non-toxicity, chemical and thermal stability.[1-5] Particularly cerium doped YAG phosphor (YAG:Ce^{3+}) emitting yellow light with a fairly broad spectral power distribution become the most commonly used phosphor in commercial white light emitting diode (WLED) for solid-state lighting because of their many advantages, including long lifetime, easy fabrication, environment friendly and low cost.[6-10] By incorporating YAG:Ce^{3+} phosphor in the body of a blue light 460 nm InGaN LED, some of the blue light will be converted into yellow light by the phosphor.[11, 12] The remaining blue light, when mixed with the yellow light, results in white light.[13, 14] In this case, the efficiency of WLED is mostly depended on the performance of YAG:Ce^{3+} phosphor. However, the main drawback of the YAG:Ce^{3+}-based WLEDs is low conversion efficiency.[15] At low amount of YAG:Ce^{3+} phosphor, phosphor only emits weak yellow light due to low quantum efficiency (QE) which is not enough to efficiently convert into white light. In this connection, increasing the amount of YAG:Ce^{3+} phosphor seems to be one of the few options to emit more yellow light which can be converted into white light, however the larger amount of phosphor used will decrease the efficiencies of WLEDs due to stronger re-absorption of light and more substantial backscattering of the emission.[16-18] Moreover, the YAG:Ce^{3+}-based WLEDs produce a cool white light due to the fact that YAG:Ce^{3+} have deficiency of generating red light. That results in low colour rendering index (CRI). Enormous research efforts were undertaken to improve red emission by co-doping red emitting rare-earth ions such as Cr^{3+}, Pr^{3+}, Sm^{3+}, and Mn^{2+}, or by mixing with red emitting phosphors or quantum dots (QDs).[19-24] However, to date, few red emitting materials with environmental friendship that can be directly excited by blue light are available. One of compromise solution is to be excited by yellow light YAG:Ce^{3+} phosphor. Therefore, it is of great importance for a given low-amount YAG:Ce^{3+} phosphor with high quantum efficiency to obtain higher conversion efficiency that will allow the production of phosphor-converted white light to meet the industrial needs.

Directly integrating plasmonic metal nanoparticles into various optoelectronic devices is believed to be the one promising approach for enhancing the performance of optoelectronic devices because plasmonic nanoparticles can generate intense localized electromagnetic fields.[25-30] By judiciously controlling the size, shape and amount of palsmonic nanoparticles loading, the device‘s efficiencies can be effectively improved.[31-36] For instance, the efficiency of InGaN/GaN-based near-ultraviolet, blue and green LEDs could be enhanced when plasmonic nanoparticles are directly deposited on the surface or embedded into the quantum well layer by physical evaporation.[37-43] Plasmonic nanoparticles can enhance the spontaneous emission and recombination of electron-hole pairs in the quantum wells.[42] Plasmon-enhanced phosphor-converted WLEDs by metal nanoparticles has not yet been explored, though plasmon-enhanced photoluminescence (PL) in YAG:Ce^{3+} thin film has already been observed by the physical deposition of silver nano-islands.[44] However, plasmonic nano-patterned structures prepared by physical evaporation are not feasible. For phosphor-converted WLED, the most adopted process is to deposit a layer composed of low-amount phosphor powder and epoxy resin (serving as the encapsulation) on the blue LED chip. Note that there is a two-fold undesired consequence to incorporate the plasmonic nanostructures in such process: First, one may need additional steps to planarize the resin to facilitate the deposition of metallic nano-patterns; Second, the presence of metallic structures will further degrade the transparency, which is not good for white light emitting purpose.[45-47] Therefore, one of the most accessible solutions is to chemically attach the plasmonic nanoparticles directly with phosphor micro-particles which are then immersed within the encapsulation resin. Since such step could be one stand-alone process before painting onto blue InGaN chips, it may greatly benefit the robust and efficient mass production in the future. Nevertheless, the small usage of phosphor as pointed out previously imposes a great challenge in producing high-quality white light emission in phosphor-converted WLED industry, we propose and experimentally demonstrate the current chemical preparation method to attach Au nanoparticles onto YAG:Ce^{3+} phosphor directly, which yields efficient and quality conversion of blue light to yellow conversion in the presence of low amount of phosphor. Au nanoparticles directly attached on the surface of YAG:Ce^{3+} nanoparticles strongly enhance local electromagnetic field of Au nanoparticles on phosphor particles. The plasmon enhancement results in effective improvement of conversion efficiency of low-amount YAG:Ce^{3+} in WLEDs device by the influence of Au nanoparticle on the radiative and non-radiative energy transfer for Ce^{3+} 5d level, leading to better white light emission.

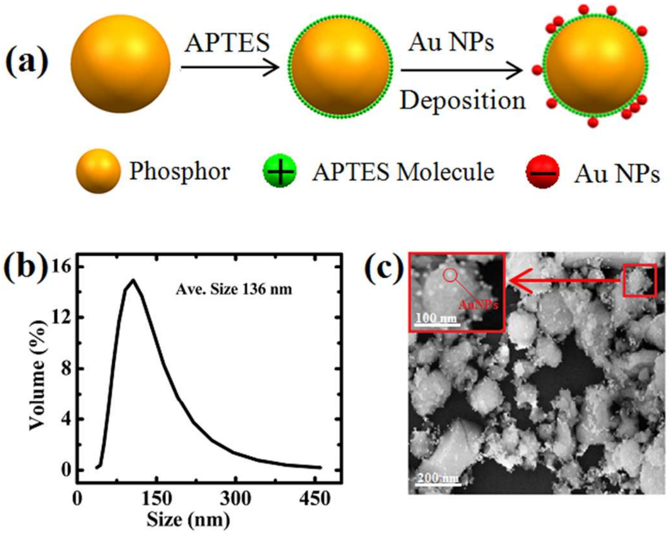

Fig. 1 (a) The Schematic diagram shows the functionalization of YAG:Ce^{3+} by APTES and modification of YAG:Ce^{3+} with Au nanoparticles (Au NPs); (b) Particle size distribution of YAG:Ce^{3+}; (c) SEM image of YAG:Ce^{3+} modified with Au nanoparticles.

In a typical experiment, as sketched in Fig. 1a, 3-Aminopropyltriethoxysilane (APTES) is used as the binding molecule for the modification of Au nanoparticles on the surface of YAG:Ce^{3+} phosphors.[48] APTES covalently attaches to the surface of YAG:Ce^{3+} phosphor and provides uniform and positively charged amine groups on the surface. These groups in turn attract the negatively charged citrate-stabilized Au nanoparticles when adding YAG:Ce^{3+} phosphor into the colloidal Au nanoparticles solution.[49] Before the surface modification with APTES, YAG:Ce^{3+} powder is grinded by using alumina mortar and pestle and measured by dynamic light scattering (DLS). Fig. 1b shows that YAG:Ce^{3+} nanoparticles have an average size of 136 nm after grinding. The Au nanoparticles were synthesized by sodium citrate reduction of HAuCl$_4$ solution and have a uniform size of 21 nm (see supporting information, Fig. S1). The surface morphology of YAG:Ce^{3+} with Au (YAG:Ce^{3+}/Au) nanoparticles confirmed by scanning electron microscope (SEM) is shown in Fig. 1c. It is found that Au nanoparticles are well attached to the surface of YAG:Ce^{3+} nanoparticles with individual particle and small aggregates of Au. The material composition analysis of YAG:Ce^{3+}/Au nanoparticles carried out with energy-dispersive X-ray (EDX) spectroscopy also shows the good purity of YAG:Ce^{3+} with Au nanoparticle (Fig. S2). All above results confirm unambiguously the successful functionalization of Au nanoparticles onto these YAG: Ce^{3+} nanoparticles.

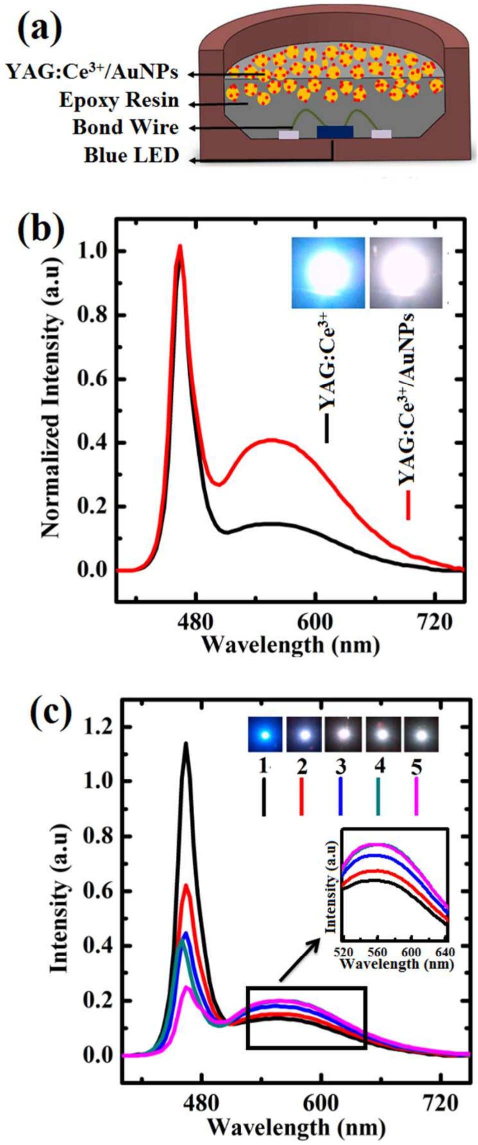

Fig. 2 (a) Schematic illustration of phosphor converted WLED device structure; (b) The Electroluminescence spectra of blue light InGaN pumped WLED based on YAG:Ce^{3+} with and without Au

nanoparticles and their corresponding photograph; (c) Amount-dependent electroluminescence spectra of YAG:Ce$^{3+/}$Au nanoparticles based WLEDs and their corresponding photograph (1: 1.39 mg/cm^2, 2: 1.99 mg/cm^2, 3: 3.36 mg/cm^2, 4: 4.43 mg/cm^2, 5: 5.18 mg/cm^2)

WLEDs was fabricated by combining surface-mounting device typed InGaN-based blue emitting LEDs (λem = 460 nm) with the same amount of pure YAG:Ce^{3+} or YAG:Ce^{3+}/Au nanoparticles embedded with epoxy resin (Fig. 2a). Fig. 2b shows the Electroluminescence (EL) spectra of pure YAG:Ce^{3+} (black colour curve) and YAG:Ce^{3+}/Au nanoparticles (red colour curve) based WLEDs. The performance of YAG:Ce^{3+} converted WLED depends on the maximum energy conversion from the pumped blue light to the phosphor. In Fig. 2b, we normalize EL spectra of LED with YAG:Ce^{3+}/Au nanoparticles at 460 nm, the peak ratio (Peak550nm/Peak460nm) is much higher than that of LED with pure YAG:Ce^{3+}. It indicates that the energy conversion from the pumped blue light to YAG:Ce^{3+} improves, which can be attributed to the plasmonic effect of Au nanoparticles. At low amount of pure YAG:Ce^{3+} (3.36 mg/cm^2), the Commission International de l'Eclairage (CIE) [50] coordinates of (0.23, 0.23) show the device still emit blue light due to the low conversion efficiency of YAG:Ce^{3+}. After Au nanoparticles modification, the CIE colour coordinates move to white light region (0.30, 0.33), which indicates Au nanoparticles effectively improve the conversion efficiency of low-amount YAG:Ce^{3+} in WLEDs. It exhibits Correlated Colour Temperature (CCT) value of 6601 K and good white light CRI value of 78. We further increase the amount of pure YAG:Ce^{3+} nanoparticle to 5.18 mg/cm^2 for emitting more yellow light, which can also get white light with similar CIE color coordinates. Therefore, we can reduce around 35% amount of YAG:Ce^{3+} nanoparticles in WLEDs.

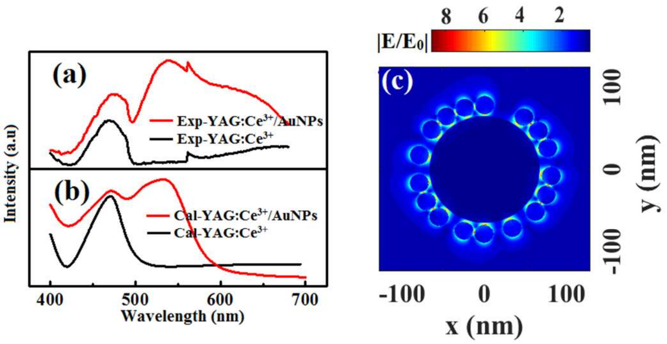

Fig. 3 (a) The experimental and (b) simulated UV-visible absorption spectra of YAG:Ce^{3+} and YAG:Ce$^{3+/}$Au nanoparticles; (c) FDTD simulated electric profile of Au nanoparticles randomly distributed on the surface of the phosphor at Au nanoparticles absorption peak 536 nm.

To clarify the plasmonic effect of Au nanoparticles for YAG:Ce^{3+} phosphor, a further study is conducted by UV-Visible spectroscopy (Fig. 3a). The absorption band peak at 468 nm is contributed from the YAG:Ce^{3+}. The additional peak of YAG:Ce^{3+}/Au nanoparticle (weight ratio = 100:5.5) at 536 nm is caused by surface plasmon resonance of the Au nanoparticle.[51]. Indeed, theoretically calculated optical properties of YAG:Ce^{3+}/Au nanoparticles using finite-difference time-domain (FDTD) method (Lumerical Solutions, Inc.) confirm the presence of the two major bands YAG:Ce^{3+}/Au nanoparticles (Fig. 3b). Both experimental and simulation results agreed with each other. Fig. 3c and S3 depict the simulation of the electric field profile of the YAG:Ce^{3+} nanoparticle with and without Au nanoparticle at Au absorption peak 536 nm. The coupling of the Au nanoparticle at the surface is expected to strongly affect the local surface electromagnetic field profile of the phosphor nanoparticles structure. The plasmonic effect of the Au nanoparticle can be clearly seen in the contrast of electric field profiles as shown in Fig. S4, where the change in the electric field profiles with and without Au nanoparticles is depicted. It is observed that the enhanced plasmonic near fields caused by Au nanoparticles alter the local surrounding fields near the phosphor surface. Further, PL emission and time-resolved spectroscopy measurements of PL from YAG:Ce^{3+} phosphor without and with Au nanoparticles were investigated to verify the plasmonic effect of Au nanoparticles in Fig. 4. It is found that the PL emission intensity of YAG:Ce^{3+} phosphor significantly was enhanced with Au nanoparticle modification (Fig. 4a). The absolute internal PL quantum yield (QYint) of YAG:Ce^{3+} phosphor was found to be 41%. The absorption ratio and external QY (QYext) are 35% and 14%, respectively. After Au nanoparticle modification, the QYint of YAG:Ce^{3+}/Au nanoparticles reached up to 66%. The absorption ratio and external QY (QYext) are 44% and 29%, respectively. In addition, the measurements show that the addition of Au nanoparticles has reduced the decay time of the YAG:Ce^{3+} from 70.7 to 68.2 ns (Fig. 4b).[52-55] As the plasmon resonance around 536 nm of Au nanoparticles overlaps well with the YAG:Ce^{3+} phosphor luminescent band, the radiative rate can be enhanced.[54, 56, 57] The radiative rate was proportional to the QY, indicating that the increase of the radiative recombination rate by the surface plasmon resonance is the main reason for the enhancement of the PL of YAG:Ce^{3+} phosphor after Au nanoparticles modification.[58-60] . The temporal stability of WLEDs based on same amount of YAG:Ce^{3+} nanoparticles with and without Au nanoparticles were investigated with increasing operating time (Fig. 4c). After first 30 hours, the luminance of YAG:Ce^{3+} nanoparticles without Au nanoparticles starts to decline due to thermal quenching and non-radiative losses. After modification with Au nanoparticles, the luminance of WLED shows good stability, which is attributed to improvement of the radiative recombination rate of YAG:Ce^{3+} under the plasmonic effect of Au nanoparticles.

Fig. 2c shows EL spectra of WLEDs fabricated with YAG:Ce^{3+}/Au nanoparticles with increasing amount from 1.39 mg/cm^2 to 5.18 mg/cm^2. It is found that the absorption of blue (460 nm) excitation light increases when increasing the particle amount which results in the enhancement of PL intensity of YAG:Ce^{3+} due to the plasmonic effect of Au nanoparticle. Table S1 summarized the parameters of YAG:Ce^{3+}/Au nanoparticles based WLEDs at different particle amount. The CIE coordinates, CRI, CCT and luminous efficiency (LE) values of WLEDs are improved when increasing the particle amount to 4.43mg/cm^2. These results suggest Au nanoparticles can improve the conversion efficiency of YAG:Ce^{3+} with increasing the amount of YAG:Ce^{3+}/Au nanoparticles. However, PL intensity of YAG:Ce^{3+} doesn't increase further and a decrease in performance of WLED was observed at higher amount of particles (5.18 mg/cm^2), because nonradiative recombination occurs when Au nanoparticles is in close proximity each other due to the resulting destructive interference of the surface plasmons.[61]

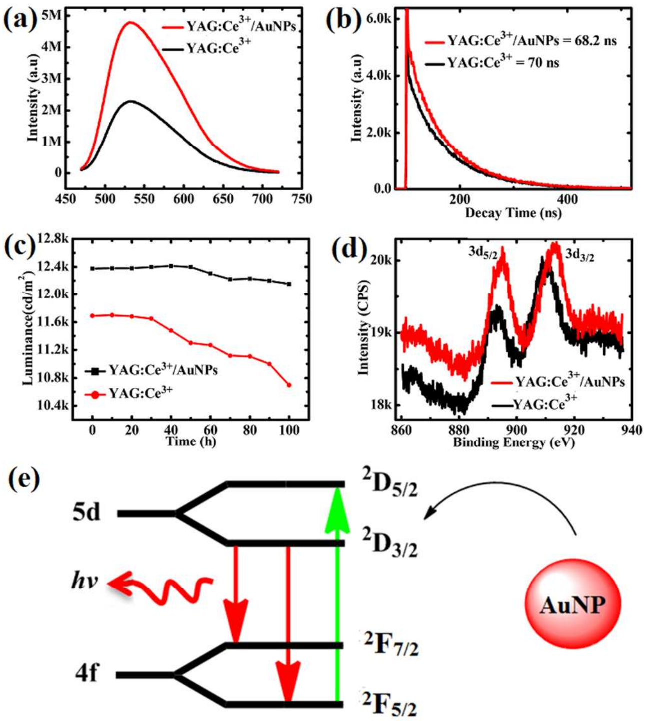

Fig. 4 (a) PL spectra of YAG:Ce^{3+} and YAG:Ce^{3+}/Au nanoparticles; (b) Time resolved spectroscopic PL measurements of YAG:Ce^{3+} and YAG:Ce^{3+}/Au nanoparticles; (c) Temporal evolution of luminance of YAG:Ce^{3+} and YAG:Ce^{3+}/Au nanoparticles white LEDs operated for a prolonged duration up to 100 h; (d) Ce (3d) XPS spectra of YAG:Ce^{3+} and YAG:Ce^{3+}/Au nanoparticles; (e) The schematic illustration of plasmonic effect of the Au nanoparticle for YAG:Ce^{3+} along with possible transitions in YAG:Ce^{3+}.

It is known that the blue excitation light (460 nm) is used to excite YAG:Ce^{3+} in Ce^{3+} doped YAG converted WLED system, which can cause Ce^{3+} $^2F_{5/2}$ (or $^2F_{7/2}$) to Ce^{3+} $^2D_{5/2}$ transitions.[62] The electrons at the $^2D_{5/2}$ excited level are unstable and non-radiatively decay to $^2D_{3/2}$ due to electron phonon interaction.[62] Consequently, the yellow luminescence is associated by Ce^{3+} $^2D_{3/2}$ to $^2F_{7/2}$ or $^2F_{5/2}$ transitions. Fig. 4d shows X-ray photoelectron spectroscopy (XPS) of YAG:Ce^{3+} phosphor and Au nanoparticle before and after modification. The binding energy of 893.0 eV and 909.8 eV represents Ce^{3+} 3d$_{5/2}$ and 3d$_{3/2}$ states, respectively.[63] After modification of Au nanoparticles, the binding energy of Ce^{3+} 3d$_{5/2}$ and 3d$_{3/2}$ significantly shift to higher energy, which is attributed to the plasmonic effect of Au nanoparticles to the 5d level of Ce^{3+}. It further confirms the influence of Au nanoparticle on the radiative and non-radiative energy transfer from 5d level, which results in the improvement of the QY of YAG:Ce^{3+}. Moreover, the binding energies at 84.30 eV and 87.90 eV are correspondence to 4f$_{7/2}$ and 4f$_{5/2}$ states of Au nanoparticles (Fig. S5). After attached to the surface of YAG:Ce^{3+} nanoparticles, binding energy of Au 4f$_{7/2}$ and 4f$_{5/2}$ shifts to higher values that demonstrates the strong interaction between Au nanoparticles and YAG:Ce^{3+}.[64] Based on the above discussions, the energy level diagram for the Ce^{3+} in YAG affected by Au nanoparticles is represented in Fig. 4e.[31, 65, 66]

Experimental Section

The YAG:Ce^{3+} ($Ce_{0.06}Y_{2.94}Al_5O_{12}$) powder sample was synthesized by conventional high temperature solid state reaction method. The 99.99% pure mixture of Al_2O_3, Y_2O_3 and CeO_2 were ground for 1h, followed by a heating process at 900°C for 3 h. After cooling to room temperature, the powders were reground to improve the mixture. Then the powders were moved into the furnace of 1660°C for 10 h. During the 10h heating process, the gas mixture of H_2 and N_2 were introduced to avoid the emerging of Ce^{4+} ions, which are hardly excited by the UV/blue photons. Finally, we got the particle size distribution D50 = 15 μm. In order to reduce the size to nano meter, we took the 0.05g YAG:Ce^{3+} nanoparticles in the mortar and manually grinded it by using pestle for 6 hours. The color of phosphor powder changed from yellow to off white or milky. The YAG:Ce^{3+} nanoparticles were functionalized by APTES purchased from J&K Scientific Ltd. 0.01g powder of YAG:Ce^{3+} nanoparticles were mixed with 450 ml absolute ethanol and 0.5ml APTES, and kept stirring at room temperature. After 90 minutes, the sample were centrifuged and rinsed by DI water. Then dispersed them into 2ml solution of Au nanoparticles (21 nm, 0.275mg/ml) and kept shaking at room temperature for 24 hours. The YAG:Ce^{3+}/Au weight ratio is around 100:5.5 (55mg of Au nanoparticles/g of YAG:Ce^{3+} phosphor). The average size of the Ce-doped phosphor material particle distribution is analysed by dynamic light scattering (DLS) method (Malvern Instrument, Model ZEN3690). The material composition and morphology are examined by scanning electron microscope (Carel Zeiss Microscopy) that also includes an energy dispersive X-ray spectrometer (Oxford Instruments, Model 51-XMX1004). The PL spectra is measured using fluorescence spectrometer "Fluoromax-4" with Xe lamp under excitation wavelength 450 nm and PL decay time by NanoLED-455 nm laser having pulse duration 1.4 ns (HORIBA JobinYvon). Absolute quantum yields were measured using a quanta-phi integrated sphere module equipped in a Fluoromax-4 spectrophotometer. The absorption spectra are recorded by UV/visible spectrometer (Lambda 750 PerkinElmer). The binding energy of Ce^{3+} in YAG:Ce^{3+} and YAG:Ce^{3+}/Au nanoparticle is measured by X-ray photoelectron spectroscopy (Kratos Analytical Shimadzu Group Company).

The WLED of YAG:Ce^{3+} and YAG:Ce^{3+}/Au nanoparticle embed with epoxy resin is fabricated and pumped by 460 nm InGaN blue LED under remote configuration. Different amount of YAG:Ce^{3+}/Au nanoparticles (0.062mg, 0.089mg, 0.150mg, 0.198mg, and 0.231mg) mixed with epoxy resin (1mg) were coated on the LED chip by using dispensing method. The LED optical properties are measured by Spectrometer (Photo Research Inc. Model PR-655) connected with Keithley 2400s source meter. All the mentioned measurements are performed at room temperature. The interaction between the localized plasmons from the Au nanoparticle and the YAG:Ce^{3+} has been numerically calculated by a using a commercial FDTD solver (Lumerical FDTD Solutions). The YAG:Ce^{3+} and Au optical properties are modelled according to our UV/visible optical measurements and also established experimental sources.[67, 68] In order to closely model the experimental setup. The YAG:Ce^{3+}/Au nanoparticle system is modelled as a periodic structure with a unit cell of 250 by 250 nm consisting of a spherical YAG:Ce^{3+} particle with a radius of 68 nm coupled with Au nanoparticle of 10.5 nm in radius. The sizes of the YAG:Ce^{3+} and Au nanoparticles have been selected based on DLS measurements. In order to uniformly excite the structure, a circularly polarized light has been used as the source. The total absorption in the structure has been calculated in the visible spectra range.

Conclusions

In summary, we present an approach for using low-amount of YAG:Ce^{3+} to convert white light by directly chemical modification of Au nanoparticles on the surface of YAG:Ce^{3+} nanoparticle. PL intensity and QY of YAG:Ce^{3+} phosphor in WLEDs are significantly enhanced after Au nanoparticle modification due to the improvement of energy conversion from the pumped blue light to YAG:Ce^{3+}, which can be attributed to strongly enhanced local surface electromagnetic field of Au nanoparticles on phosphor particle surface. FDTD simulation, time-resolved spectroscopy, and XPS data unanimously verify the plasmonic effect of Au nanoparticle to YAG:Ce^{3+} phosphor. The radiative and non-radiative energy transfer from Ce^{3+} 5d level is directly affected by the surface plasmon of Au NPs, resulting in the improvement of CIE coordinates, CCT and CRI of YAG:Ce$^{3+/}$Au nanoparticles based WLED. Our work not only demonstrates that employing plasmonic nanoparticle can improve the conversion efficiency of phosphor, but also provides a very promising way to develop high efficiency phosphor-converted WLEDs as a solid-state light source. The Au nanoparticle modification route should be applicable to various converting materials, and will facilitate the formation of many converters/Au composites leading to new and intriguing properties and applications.

Acknowledgements

This work was supported by National Natural Science Foundation of China (Project Code, 21373144), the Natural Science Foundation of Jiangsu Province of China (Grant No. BK2011033, BK20130287 and BK20140353), and the 56th class General Financial Grant from the China Postdoctoral Science Foundation (2014M561704). This is also a project funded by the Priority Academic Program Development of Jiangsu Higher Education Institutions (PAPD). C.W. Qiu would like to acknowledge the financial support from National University of Singapore (Grant Number: R-263-000-A45-112). H. Q. Ye would like to thank for the supports of Jiashan Economic Development Zone Post-Doctoral Working Station, Zhejiang Province and Jiashan Forever Green Chem. Tech. Co., Ltd.

Notes and references

[a] National Astronomical Observatories / Nanjing Institute of Astronomical Optics & Technology, Key Laboratory of Astronomical Optics & Technology, Nanjing Institute of Astronomical Optics & Technology, Chinese Academy of Sciences, Nanjing, Jiangsu, 210042, P. R. China.

[b] Institute of Functional Nano & Soft Materials (FUNSOM), Jiangsu Key Laboratory for Carbon-based Functional Materials and Devices & Collaborative Innovation Center of Suzhou Nano Science & Technology, Soochow University, Suzhou, Jiangsu 215123, P. R. China.

E-mail: ljiang@suda.edu.cn; chilf@suda.edu.cn

[c] Department of Electrical and Computer Engineering, National University of Singapore, 4 Engineering Drive 3, Singapore 117576, Singapore.

[d] School of Electronic Science & Engineering, Southeast University, Nanjing, 210096, P.R. China.

[e] University of Chinese Academy of Sciences, Beijing, 100049, P. R. China.

1. P. B. Oliete, J. I. Peña, A. Larrea, V. M. Orera, J. Llorca, J. Y. Pastor, A. Martín and J. Segurado, *Adv. Mater.*, 2007, 19, 2313-2318.
2. X. Huang, *Nat. Photonics*, 2014, 8, 748-749.
3. E. F. Schubert and J. K. Kim, *Science*, 2005, 308, 1274-1278.
4. P. Seiler, K. Wallmeroth and K. Mann, *Nat. Photonics*, 2010, 4, 285-285.
5. T. Klink, G. Schlunck, W. E. Lieb, J. Klink and F. Grehn, *Eye*, 2006, 22, 370-374.
6. M. L. Saladino, D. Chillura Martino, M. A. Floriano, D. Hreniak, L. Marciniak, W. Stręk and E. Caponetti, *J. Phys. Chem. C*, 2014, 118, 9107-9113.
7. S. Ye, F. Xiao, Y. X. Pan, Y. Y. Ma and Q. Y. Zhang, *Mater. Sci. Eng. R*, 2010, 71, 1-34.
8. J. Dwivedi, P. Kumar, A. Kumar, Sudama, V. N. Singh, B. P. Singh, S. K. Dhawan, V. Shanker and B. K. Gupta, *RSC Adv.*, 2014, 4, 54936-54947.
9. E. C. W. Ou, L. Hu, G. C. R. Raymond, O. K. Soo, J. Pan, Z. Zheng, Y. Park, D. Hecht, G. Irvin, P. Drzaic and G. Gruner, *ACS Nano*, 2009, 3, 2258-2264.
10. C. Wang, R. Bao, K. Zhao, T. Zhang, L. Dong and C. Pan, *Nano Energ.*
11. B. Chen, H. Zhong, M. Wang, R. Liu and B. Zou, *Nanoscale*, 2013, 5, 3514-3519.
12. W.-S. Song, J.-H. Kim, J.-H. Lee, H.-S. Lee, Y. R. Do and H. Yang, *J. Mater. Chem.*, 2012, 22, 21901-21908.
13. P. Schlotter, R. Schmidt and J. Schneider, *Appl. Phys. A*, 1997, 64, 417-418.
14. H. S. Jang, Y. H. Won and D. Y. Jeon, *Appl. Phys. B*, 2009, 95, 715-720.
15. W. B. Im, N. George, J. Kurzman, S. Brinkley, A. Mikhailovsky, J. Hu, B. F. Chmelka, S. P. DenBaars and R. Seshadri, *Adv. Mater.*, 2011, 23, 2300-2305.
16. R. Kasuya, A. Kawano, T. Isobe, H. Kuma and J. Katano, *Appl. Phys. Lett.*, 2007, 91, 111916.
17. T. Isobe, *ECS J. Solid State Sci. Technol.*, 2013, 2, R3012-R3017.
18. W.-S. S. Ho-June Byun, Yong-Seog Kim and Heesun Yang, *J. Phys. D: Appl. Phys.*, 2010, 43, 195401.
19. Y.-C. Pu and Y.-J. Hsu, *Nanoscale*, 2014, 6, 3881-3888.
20. L. Guo, Y. Wang, Y. Wang, J. Zhang, P. Dong and W. Zeng, *Nanoscale*, 2013, 5, 2491-2504.
21. H. S. Jang, W. B. Im, D. C. Lee, D. Y. Jeon and S. S. Kim, *J. Lumin.*, 2007, 126, 371-377.
22. X. Wang, X. Yan, W. Li and K. Sun, *Adv. Mater.*, 2012, 24, 2742-2747.
23. H. S. Jang, H. Yang, S. W. Kim, J. Y. Han, S.-G. Lee and D. Y. Jeon, *Adv. Mater.*, 2008, 20, 2696-2702.
24. A. Aboulaich, M. Michalska, R. Schneider, A. Potdevin, J. Deschamps, R. Deloncle, G. Chadeyron and R. Mahiou, *ACS Appl. Mater. Interfaces*, 2013, 6, 252-258.
25. L. Jiang, Y. Tang, C. Liow, J. Wu, Y. Sun, Y. Jiang, Z. Dong, S. Li, V. P. Dravid and X. Chen, *Small*, 2013, 9, 705-710.
26. L. Jiang, H. X. Zhang, J. Q. Zhuang, B. Q. Yang, W. S. Yang, T. J. Li and C. C. Sun, *Adv. Mater.*, 2005, 17, 2066-2070.
27. L. Jiang, W. C. Wang, H. Fuchs and L. F. Chi, *Small*, 2009, 5, 2819-2822.
28. Z. Liang, J. Sun, Y. Jiang, L. Jiang and X. Chen, *Plasmonics*, 2014, 9, 859-816.
29. H. I. Park, S. Lee, J. M. Lee, S. A. Nam, T. Jeon, S. W. Han and S. O. Kim, *ACS Nano*, 2014, 8, 10305-10312.
30. L.-B. Luo, C. Xie, X.-H. Wang, Y.-Q. Yu, C.-Y. Wu, H. Hu, K.-Y. Zhou, X.-W. Zhang and J.-S. Jie, *Nano Energ.*, 2014, 9, 112-120.

31. X. T. Wang, C. Liow, D. P. Qi, B. W. Zhu, W. R. Leow, H. Wang, C. Xue, X. D. Chen and S. Z. Li, *Adv. Mater.*, 2014, 26, 3506-3512.
32. L. Jiang, X. D. Chen, N. Lu and L. F. Chi, *Acc. Chem. Res.*, 2014, 47, 3009-3017.
33. L. Jiang, Y. X. Tang, C. H. Liow, J. S. Wu, Y. H. Sun, Z. L. Dong, S. Z. Li, V. P. Dravid and X. D. Chen, *Small*, 2013, 9, 705-710.
34. N. N. Jiang, L. Shao and J. F. Wang, *Adv Mater*, 2014, **26**, 3282-3289.
35. P. Guardia, K. Korobchevskaya, A. Casu, A. Genovese, L. Manna and A. Comin, *ACS nano*, 2013, **7**, 1045-1053.
36. Y. H. Jang, Y. J. Jang, S. T. Kochuveedu, M. Byun, Z. Lin and D. H. Kim, *Nanoscale*, 2014, 6, 1823-1832.
37. M.-K. Kwon, J.-Y. Kim, B.-H. Kim, I.-K. Park, C.-Y. Cho, C. C. Byeon and S.-J. Park, *Adv. Mater.*, 2008, 20, 1253-1257.
38. C. Y. Cho, S. J. Lee, J. H. Song, S. H. Hong, S. M. Lee, Y. H. Cho and S. J. Park, *Appl. Phys. Lett.*, 2011, 98, 051106.
39. N. Gao, K. Huang, J. Li, S. Li, X. Yang and J. Kang, *Sci. Rep.*, 2012, 2, 816.
40. K. Okamoto, I. Niki, A. Shvartser, Y. Narukawa, T. Mukai and A. Scherer, *Nat. Mater.*, 2004, 3, 601-605.
41. S.-H. Hong, C.-Y. Cho, S.-J. Lee, S.-Y. Yim, W. Lim, S.-T. Kim and S.-J. Park, *Opt. Express*, 2013, 21, 3138-3144.
42. A. Neogi, C.-W. Lee, H. O. Everitt, T. Kuroda, A. Tackeuchi and E. Yablonovitch, *Phys. Rev. B*, 2002, 66, 153305.
43. T. S. Oh, H. Jeong, Y. S. Lee, J. D. Kim, T. H. Seo, H. Kim, A. H. Park, K. J. Lee and E.-K. Suh, *Appl. Phys. Lett.*, 2009, 95, 111112.
44. W.-H. Chao, R.-J. Wu, C.-S. Tsai and T.-B. Wu, *J. Appl. Phys.*, 2010, 107, 013101.
45. X.-F. Zeng, X.-R. Kong, J.-L. Ge, H.-T. Liu, C. Gao, Z.-G. Shen and J.-F. Chen, *Ind. Eng. Chem. Res*, 2011, 50, 3253-3258.
46. O. Parlak and M. M. Demir, *ACS Appl. Mater. Interfaces*, 2011, 3, 4306-4314.
47. A. Dang, S. Ojha, C. M. Hui, C. Mahoney, K. Matyjaszewski and M. R. Bockstaller, *Langmuir*, 2014, 30, 14434-14442.
48. A. R. Morrill, D. T. Duong, S. J. Lee and M. Moskovits, *Chem. Phys. Lett.*, 2009, 473, 116-119.
49. J. A. Howarter and J. P. Youngblood, *Langmuir*, 2006, 22, 11142-11147.
50. CIE, *Commission Internationale de l'Eclairage Proceedings* 1931, Cambridge University Press, Cambridge. .
51. P. K. Jain, K. S. Lee, I. H. El-Sayed and M. A. El-Sayed, *J. Phys. Chem. B*, 2006, 110, 7238-7248.
52. W. Ge, X. Zhang, M. Liu, Z. Lei, R. Knize and Y. Lu, *Theranostics*, 2013, 3, 282.
53. J. R. Lakowicz, *Anal. Biochem.*, 2005, 337, 171-194.
54. S. Schietinger, T. Aichele, H.-Q. Wang, T. Nann and O. Benson, *Nano Lett.*, 2009, 10, 134-138.
55. P. Wang, X. Zhao and B. Li, *Nano Energ.*, 2012, 1, 152-158.
56. R. Esteban, M. Laroche and J.-J. Greffet, *J. Appl. Phys.*, 2009, 105, 033107.
57. S. Sapra, S. Mayilo, T. A. Klar, A. L. Rogach and J. Feldmann, *Adv. Mater.*, 2007, 19, 569-572.
58. J.-H. Song, T. Atay, S. Shi, H. Urabe and A. V. Nurmikko, *Nano Lett.*, 2005, 5, 1557-1561.
59. B. Peng, Z. Li, E. Mutlugun, P. L. Hernandez Martinez, D. Li, Q. Zhang, Y. Gao, H. V. Demir and Q. Xiong, *Nanoscale*, 2014, 6, 5592-5598.
60. T. Nychyporuk, Y. Zakharko, T. Serdiuk, O. Marty, M. Lemiti and V. Lysenko, *Nanoscale*, 2011, 3, 2472-2475.
61. D.-R. Jung, J. Kim, S. Nam, C. Nahm, H. Choi, J. I. Kim, J. Lee, C. Kim and B. Park, *Appl. Phys. Lett.*, 2011, 99, 041906.
62. L. Chen, C.-C. Lin, C.-W. Yeh and R.-S. Liu, *Materials*, 2010, 3, 2172-2195.
63. L. T. Su, A. I. Y. Tok, F. Y. C. Boey, X. H. Zhang, J. L. Woodhead and C. J. Summers, *J. Appl. Phys.*, 2007, 102, 083541.
64. B. A. F. Kengne, S. Karmakar, M. Kaura, V. V. R. Sai, G. Corti, I. B. Niraula, A. Larin, J. Hall, D. Sowell, P. J. Hrdlicka, V. Dobrokhotov and D. N. McIlroy, *Acs Appl. Mater. Inter.*, 2014, **6**, 13355-13366.
65. P. Dorenbos, *Phys. Rev. B*, 2012, 85, 165107.
66. Y. Baer and J. K. Lang, *J. Appl. Phys.*, 1979, 50, 7485-7488.
67. P. B. Johnson and R. W. Christy, *Phys. Rev. B*, 1972, 6, 4370-4379.
68. D. E. Zelmon, D. L. Small and R. Page, *Appl. Opt.*, 1998, 37, 4933-4935.